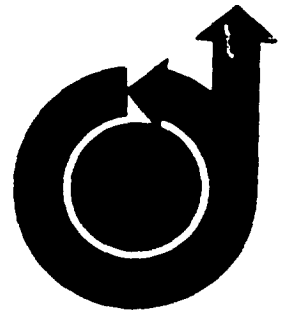


71225

Clark

**AIAA** Paper  
No. **69-396**



THE DESIGN OF **HYDROFILL** CROSS SECTIONS AS A FUNCTION OF  
CAVITATION NUMBER, LIFT, AND STRENGTH

by

THOMAS G. LANG  
Naval ~~Undersea~~ Research and **Development** Center  
San Diego, California

**AIAA**  
**2nd Advanced Marine Vehicles**  
**and Propulsion Meeting**

SEATTLE, WASHINGTON/MAY 21-23, 1969

First publication rights reserved by American Institute of Aeronautics and Astronautics, 1290 Avenue of the Americas, New York, N. Y. 10019.  
Abstracts may be published without permission if credit is given to author and to AIAA. (Price: AIAA Member \$1.00, Nonmember \$1.50)

10-00 2496

**THE DESIGN OF HYDROFOIL CROSS SECTIONS AS A FUNCTION OF  
CAVITATION NUMBER, LIFT, AND STRENGTH**

Thomas G. Lang, PhD  
Naval Undersea Research and Development Center  
San Diego, California

Abstract

A set of graphs and equations is developed for quickly determining the **minimum-drag** form of **non-cavitating** and **supercavitating** hydrofoils designed for high Reynolds numbers where the **boundary** layer is fully turbulent. A single classification parameter is derived which simplifies design selection. The results are applicable to the design of propellers, **struts**, lifting surfaces, and fins for both submerged vehicles and surface craft. It is shown that hydrofoil cross sections can be classified into **six** basic types of design forms, five of which are cavitating.

List of Symbols

(Dimensions are in force F, length L, and time T)

b	Hydrofoil span (L)
c	Chordlength of a hydrofoil (L)
$C_d$	Hydrofoil drag coefficient = $D/\rho U^2 bc/2$
$C_{dc}$	Cavity drag coefficient
$C_{d0}$	Cavity drag coefficient when $\sigma = 0$
$C_f$	Skin friction drag coefficient
$C_L$	Lift coefficient = $L/\rho U^2 bc/2$
$C_{L0}$	Lift coefficient at $a = 0$ ; $C_{L0} = C_L - 2a$
$C_1$	Section modulus coefficient = $2I/t^3 c$
D	Hydrofoil drag (F)
$D_c$	Cavity drag of a hydrofoil (F)
f	<b>Design</b> bending stress, including load factor and factor of safety ( $FL^{-2}$ )
I	Area moment of <b>inertia</b> ( $L^4$ )
k	Designates the amount of camber of a 2-term hydrofoil camber line
K	<b>Hydrofoil classification parameter</b> = $(\sigma \cdot C_L/2)/\sqrt{M^*} = \sigma_0/\sqrt{M^*} = -C_{L0}/2\sqrt{M^*}$
$t_c$	<b>Length</b> of a cavity (L)
L	Hydrofoil lift (F)
M	Applied bending <b>moment</b> about some <b>cross</b> section of a hydrofoil (FL)
$M'$	$M/fc^3$
P	Free-stream pressure ( $FL^{-2}$ )
$P_v$	<b>Vapor</b> pressure of the fluid ( $FL^{-2}$ )
$P_1$	<b>Minimum</b> pressure on a hydrofoil ( $FL^{-2}$ )
r	Characteristic roughness height (L)
$r'$	$r/c$
R	Reynolds number = $Uc/\nu$
t	<b>Maximum thickness</b> of a hydrofoil (L)
$t'$	$t/c$
a	Hydrofoil base thickness (L)

\*The numbers in parenthesis denote references which are listed at the end of this paper.

$t_c$	<b>Maximum thickness</b> of a cavity (L)
U	Free-stream velocity ( $LT^{-1}$ )
$U_1$	Velocity at the <b>minimum</b> pressure point on a hydrofoil ( $LT^{-1}$ )
x	<b>Chordwise</b> distance to a specific point on a hydrofoil from its leading edge (L)
$x'$	$x/c$
Y	Distance from the chordline to a specific point on a hydrofoil surface (L)
$Y'$	$y/c^3$
$y'_l(x')$	Local nondimensional lower surface height above the chordline
$y'_m(x')$	Local nondimensional <b>meanline</b> height above the chordline
$y'_o(x')$	Nondimensional <b>meanline</b> of the NACA uniform pressure ( $a = 1.0$ ) <b>meanline</b> designed for a unit lift coefficient
$y'_u(x')$	<b>Local</b> nondimensional upper surface height above the chordline
$y'_1$ to 5	Nondimensional heights of hydrofoil parameters listed in Table 2
$\epsilon$	Angle of attack used for generating thickness for a supercavitating hydrofoil (radians),
$\nu$	Kinematic viscosity of the fluid ( $L^2T^{-1}$ )
$\rho$	Mass density of the <b>fluid</b> ( $FL^{-4}T^2$ )
a	Cavitation number = $\frac{P - P_v}{\rho U^2/2}$
$\sigma_{cr}$	Incipient cavitation number, i.e., value of $\sigma$ when cavitation is about to begin as a reduces
$\sigma_0$	Represents $\sigma$ when $CL = 0$ ; $\sigma_0 = \sigma \cdot C_L/2$
$\tau$	Designates <b>amount</b> of parabolic thickness added to a hydrofoil

Terms with a bar over them are defined in Equation 37

Introduction

This paper is an abstract of the **section** titled "**The Design of Hydrofoil Cross Sections**" in the author's **PhD thesis** (1) on engineering **design** theory. Consequently, any background information and detailed explanations that have been omitted from this paper may be found in Reference (1).

Hydrofoils are found in a wide variety of **commonly** encountered situations. They are used as propeller blades on boats, as sailboat keels, ship rudders, submarine and torpedo fins, lifting surfaces of hydrofoil boats, underwater cable fairings, shroud ring stabilizers for missiles, rotor blades for water jet propulsion units, impeller blades in many kinds of pumps, support struts, etc. The many different uses of hydrofoils have resulted in the **development** of a wide variety

of hydrofoil forms. The streamlined fully-wetted hydrofoils are the most commonly encountered type, and have excellent performance characteristics at speeds up to the beginning of cavitation. Cavitation is characterized by the formation of small cavities filled with water vapor which appear and collapse in the low pressure region of the hydrofoil surface. As cavitation increases, there is a corresponding increase in the number and degree of such undesirable characteristics as noise, drag, surface pitting, reduction in lift, and unsteady performance. Cavitation can be avoided in certain situations by reducing speed, reducing the hydrofoil thickness or lift coefficient, improving the cross-sectional shape, increasing the free-stream pressure, or by operating closer to the design angle of attack of the hydrofoil.

If cavitation cannot be avoided, an entirely different type of hydrofoil can be utilized which provides steady performance, but has somewhat more drag than the best fully-wetted hydrofoils, and produces more noise. One form is called a super-cavitating hydrofoil which is analyzed by Tulin and Burkart (2) and operates with its upper surface entirely immersed in a cavity and with its lower surface fully wetted. Another form is a cavitating, non-lifting strut which is analyzed by Tulin (3) and which is entirely immersed in a cavity, except for the nose section.

A third type of hydrofoil is called a ventilated hydrofoil, various forms of which are described by Lang (4). Ventilated hydrofoils characteristically operate with a steady cavity of non-condensing gas in contact with the surface. At cavitation numbers greater than zero, this type has lower drag than a cavitating hydrofoil, and it operates more quietly. Its use requires a gas source to maintain the cavity.

For the purpose of this paper it is assumed that a gas source is not available and that the hydrofoils are either fully wetted or else designed for cavitation. Some of the advantages and disadvantages of the various hydrofoil cross sections will become evident later.

Specification of the Design Problem

Many hydrofoil design problems can be reduced to the need for a hydrofoil cross section which provides a certain lift coefficient, sustains a given bending moment, and operates well at a given cavitation number, Reynolds number, etc. The objective of this design problem is to determine the hydrofoil cross-sectional forms which have minimum drag. For simplicity, it is assumed that the flow is steady, that the only critical stress is bending stress, that all cross sections are solid, that the water surface is sufficiently far away so that it has no hydrodynamic effect, and that the angle of attack is fixed at the design angle.

Design Problem Variables. The design problem variables are assumed to be the design stress  $f$  of the structural material\*, hydrofoil chordlength  $c$ , characteristic surface roughness  $r$ , free-stream speed  $U$ , free-stream pressure  $P$ , fluid viscosity  $\nu$ ,

fluid density  $\rho$ , fluid vapor pressure  $P_v$ , lift per unit span  $L/b$ , and applied bending moment  $M$ . In summary, the ten design problem variables are  $f, c, r, U, P, \nu, \rho, P_v, L/b$ , and  $M$ . Applying the design procedure of Reference (1), the dimensional variables are reduced to five nondimensional design mission variables. These new variables characterize a nondimensional design problem, and are the lift coefficient  $C_L$ , moment coefficient  $M'$ , cavitation number  $\sigma$ , Reynolds number  $R$ , and roughness ratio  $r'$  where :

$$C_L = \frac{L/b}{c \frac{1}{2} \rho U^2} \tag{1}$$

$$M' = \frac{M}{fc^3} \tag{2}$$

$$\sigma = \frac{P - P_v}{\frac{1}{2} \rho U^2} \tag{3}$$

$$R = \frac{Uc}{\nu} \tag{4}$$

$$r' = r/c \tag{5}$$

Optimization Criterion. The objective of the nondimensional design problem is to minimize the drag coefficient  $C_d$ , where

$$C_d = \frac{D/b}{c \frac{1}{2} \rho U^2} \tag{6}$$

where  $D/b$  is the drag per unit span.

Possible Design Forms

Typical hydrofoil cross sections are sketched in Figure 1.

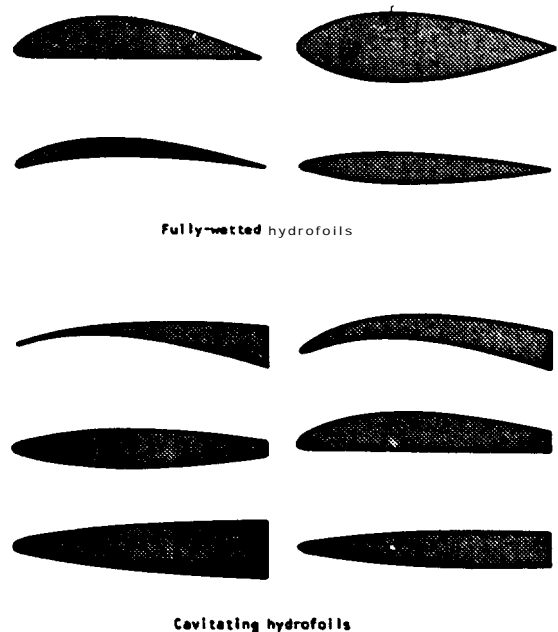


Figure 1 - Typical hydrofoil forms

\*The design stress includes the load factor and the factor of safety.

## Physical Relationships

The relationship for bending stress is considered first. The design bending stress of the minimum-drag hydrofoil cross section must be equal to the actual bending stress, so

$$f = \frac{M}{c_1 \left(\frac{t}{c}\right)^2 c^3} \quad (7)$$

where  $t$  = hydrofoil thickness, and  $c_1$  is the section modulus coefficient. Rearranging,

$$M' = \frac{M}{fc^3} = c_1 \left(\frac{t}{c}\right)^2 \quad (8)$$

Cavitation is considered next. Let  $P_1$  be the minimum pressure at some point on a fully-wetted hydrofoil where the local velocity is  $U_1$ . According to the Bernoulli equation,  $P_1$  is

$$P_1 = P + \frac{1}{2}\rho U^2 = \frac{1}{2}\rho U_1^2 = P + \frac{1}{2}\rho U^2 \left[1 - \left(\frac{U_1}{U}\right)^2\right] \quad (9)$$

Cavitation will occur when  $P_1$  reduces to the vapor pressure of the fluid  $P_v$  (assuming no tensile stress in the fluid). The critical (incipient) cavitation number is defined as

$$\sigma_{cr} = \frac{P - P_1}{\frac{1}{2}\rho U^2} = \left(\frac{U_1}{U}\right)^2 - 1 \quad (10)$$

Cavitation will occur whenever  $\sigma < \sigma_{cr}$  where  $a$  is the cavitation number.

It will now be shown that  $R$  and  $r'$  can be eliminated from the list of important variables. The Reynolds number  $R$  determines how the hydrofoil should be formed to best utilize laminar flow, prevent laminar separation, prevent turbulent separation, and minimize skin friction drag. However,  $R$  is not normally critical in the range  $R > 10^7$  because the boundary layer is generally fully turbulent, and changes in Reynolds number in this range have only a small effect on hydrofoil form. Also, it is known that the roughness ratio  $r'$  has little effect on hydrofoil form if it does not exceed certain critical values which depend upon  $R$ ; the roughness can generally be kept below these values.

In view of this discussion, it is seen that the nondimensional design problem can be simplified by assuming that  $r' = 0$  and  $R \gg 10^7$ ; the results will still be very general and useful. The design variables are consequently reduced to  $C_L$ ,  $M'$ , and  $\sigma$ . In order to approach this three-dimensional design problem, the simpler two-dimensional design problems will be considered first where one of the three variables is assumed to be zero.

### Design Problem Where $C_L = 0$

The first two-dimensional design problem is where  $C_L = 0$  and where  $M'$  and  $\sigma$  are variable. Since  $C_L = 0$ , all points in the two-dimensional problem space represented by a graph of  $\sigma$  versus  $M'$  will be satisfied by uncambered hydrofoils, called hydrofoil struts. All laminar boundary layer effects can be disregarded since the boundary layer will be fully turbulent at  $R_e \gg 10^7$ .

The problem reduces to finding the minimum drag hydrofoil strut section as a function of  $\sigma$  and  $M'$ , where the boundary layer is turbulent and  $C_f$  is very small in view of the high Reynolds number.

As shown in Reference (1), if the cavitation number is sufficiently high, an efficient fully-wetted streamlined hydrofoil can be designed to satisfy the strength requirement. However, if the cavitation number is low, the most efficient (i.e., minimum-drag) strut is bluff ended and cavitating. Consequently, the graph of  $M'$  versus  $\sigma$  will split into two regions where the upper region is satisfied by fully-wetted struts, and the lower region is satisfied by less-efficient cavitating struts.

**Fully Wetted Region.** Assuming that the fully-wetted struts have no boundary layer separation, the minimum drag form is shown by (1) to have an elliptical cross section. The pressure is theoretically approximately uniform on both surfaces from a point near the leading edge to a point near the trailing edge. Since the boundary layer will, in actual practice, separate near the trailing edge, a short cusp-shaped or wedge-shaped trailing edge can be added to the basic ellipse to minimize its drag. For the purpose of this paper, however, it will be assumed that the values of  $C_L$ ,  $\sigma$ , and  $M'$  are based upon the chordlength  $c$  of the basic elliptical section. Reference (1) shows that the stress relationship, Equation 8, for an ellipse becomes

$$(\text{ellipse}) \therefore = \sqrt{10.2 M'} \quad (11)$$

also, the cavitation relationship, Equation 10, becomes

$$(\text{ellipses}) \sigma_{cr} = 2 \frac{t}{c} \quad (12)$$

Let Region I be the portion of the  $a$  versus  $M'$  graph which is best satisfied by fully-wetted hydrofoils, and Region II be the portion which is best satisfied by cavitating hydrofoils. The boundary between the two regions is obtained from Equations 11 and 12 by letting  $\sigma_{cr} = \sigma_0$  which gives

$$(\text{Boundary between Regions I and IIa}) \sigma_0 = 6.39 \sqrt{M'} \quad (13)$$

where  $a$  designates the value of  $a$  when  $C_L$  is assumed to be zero. Equation 11 gives the ellipse ratio,  $t/c$ , as a function of  $M'$  for Region I where the form is independent of  $\sigma$ .

The drag coefficient for the Region I forms is due to skin friction only, and is shown by (1) to be

$$(\text{Region I}) \quad C_d = 2C_f(6.39 \sqrt{M'} + 1) \quad (14)$$

where  $C_f$  is the drag coefficient of a flat plate at the Reynolds number  $R$ .

**Cavitating Region.** The cavitating strut family which corresponds to Region II is shown by Reference (1) to be family of truncated ellipses where the strut lies just inside the cavity formed behind its leading edge.

The cavity drag coefficient of a full cavity is shown by (5) to be

$$C_{dc} = \frac{\pi}{8} \sigma_o^2 \frac{l_c}{c} = \frac{D_c}{bc \cdot \frac{1}{2} \rho U^2} \quad (15)$$

where  $D/b$  is the cavity drag per unit span, and  $l_c$  is the Eavity length. Assuming that  $\sigma$  is small, Reference (5) also shows that the shape of a full cavity is an ellipse,

The minimum drag strut form is a truncated ellipse and is shown by (1) to be expressed by the following relationships:

$$y' = \begin{cases} \pm \frac{\sigma_o}{2} \sqrt{\frac{2}{\sigma_o} \sqrt{\frac{M'}{C_1}} x' - (x')^2} & \text{(Region IIa)} \\ \pm \frac{\sigma_o}{2} \sqrt{\left(\frac{M'}{C_1 \sigma_o^2} + 1\right) x' - (x')^2} & \text{(Region IIb)} \end{cases} \quad (16)$$

$10.2 \leq \frac{\sigma_o^2}{M'} \leq 40.8$  (Region IIa)  
 $0 \leq \frac{\sigma_o^2}{M'} \leq 10.2$  (Region IIb)

where  $y'$  and  $x'$  are the nondimensional semi-thickness and distance from the leading edge, respectively, and where Region IIa corresponds to those struts whose chord lengths are greater than half the cavity length, and Region IIb corresponds to those struts whose chord lengths are less than half the cavity length.

Because of the mathematics involved! two different equations are required to define the strut form, and these are called regions IIa and IIb. The equation for the boundary between Regions IIa and IIb is seen from the region expressions in Equation 16 to be

$$\left( \begin{array}{l} \text{Region IIa to} \\ \text{IIb boundary} \end{array} \right) \sigma_o^2 = 10.2 M' \quad (17)$$

The value of the section modulus coefficient  $C_1$  for the two families of truncated ellipses is shown in Figure 2 as a function of the parameter  $\sigma_o^2/M'$ . This relationship was obtained by: (a) integrating over a truncated ellipse to determine the moment of inertia,  $I$ , as a function of  $c/l_c$ ; (b) calculating the value of  $C$  where  $C = 2I/t^3$ , and (c) obtaining  $\sigma_o^2/M'$  as a function of  $c/l_c$ .

The struts cavitate from their leading edges rearward because their surfaces are designed to lie just inside the cavity in order to eliminate friction drag. Their drag is therefore cavity drag only, and is obtained from Equations 15 and 16 as

$$C_d = \begin{cases} \frac{\pi}{4} \sigma_o^2 \sqrt{\frac{M'}{\sigma_o^2 C_1}} & \text{(Region IIa)} \\ \frac{\pi}{8} \sigma_o^2 \left( \frac{M'}{\sigma_o^2 C_1} + 1 \right) & \text{(Region IIb)} \end{cases} \quad (18)$$

$C_L = 0$

where  $C_1$  is obtained from Figure 2.

The upper expression of Equation 18 must be reduced somewhat to include the effect of the thrust produced by impingement of the reentry jet (which

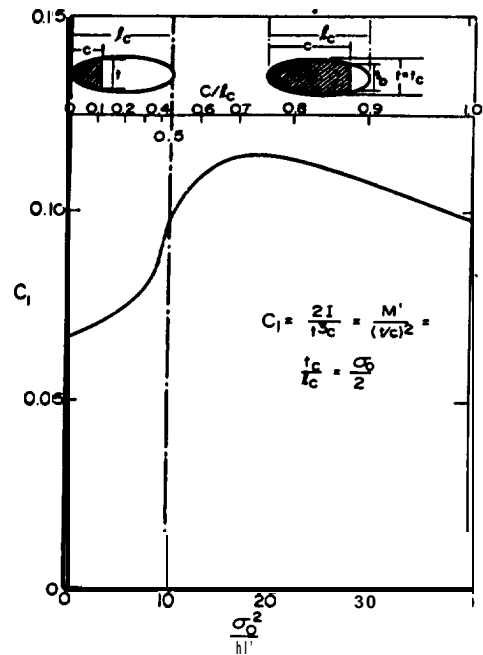


Figure 2 - Section modulus coefficient of truncated elliptical struts

exists at the rear of all cavities) on the strut trailing edge. In view of the lack of experimental data on the reentry jet effect, it is assumed that half the cavity drag is recovered as thrust when the strut almost fills the cavity, and that the effect tapers to zero recovery when the trailing edge of the cavity is located more than one-quarter of a cavity length behind the strut.

Illustration of the Design Result. Figure 3 consists of two graphs of  $C_1$  versus  $M'$  which illustrate the design result. Both graphs show the boundaries between Regions I, IIa, and IIb. Sketches of the corresponding design forms are superimposed on the lower graph at various selected points. The corresponding value of  $C_1$  is plotted on the upper graph of  $C_1$  versus  $M'$ . The dashed lines represent the regions where the reentry jet influences cavity drag.

#### Design Problem Where $M' = 0$

This two-dimensional problem is represented by a graph of  $C_1$  versus  $\sigma$ , where  $\sigma$  is selected as the abscissa. Since  $M' = 0$ , there is no strength requirement, so all forms will have minimum thickness because minimum thickness produces minimum drag. As in the previous design problem, the graph will split into a fully wetted Region I and a cavitating Region II.

Region I Consider first, the noncavitating region where  $\sigma$  is so large that cavitation will not occur. As shown in Reference (1), all minimum-drag fully-wetted hydrofoils which correspond to this region are cambered meanlines which have a uniform pressure distribution. These cambered lines are the set of NACA  $a = 1.0$  meanlines which are presented by Abbott and Doenhoff (6).

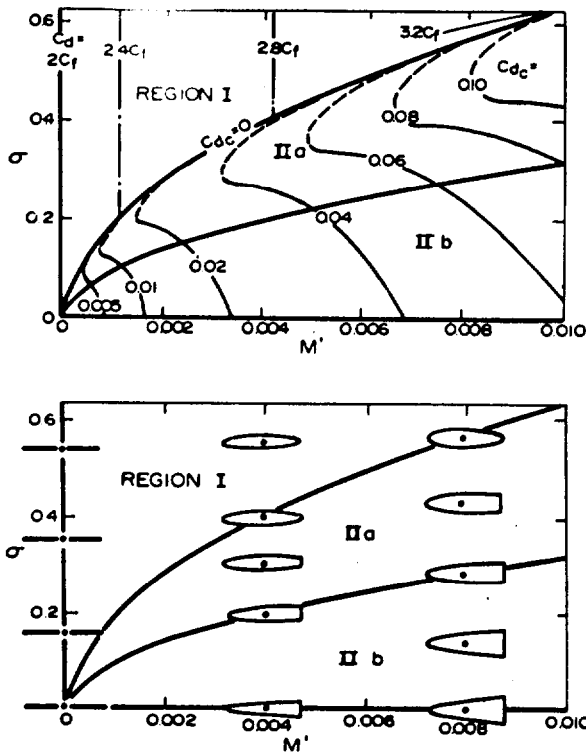


Figure 3 - Hydrofoil struts and drag coefficients for the case when  $C_L = 0$

The nondimensional meanline height is expressed as

$$y'_m(x') = y'_0(x') \cdot C_L \quad (19)$$

where  $y'_0(x')$  is the meanline height for  $C_L = 1.0$ . Some values for  $y'_0(x')$  are reproduced in Table 1 from (6).

TABLE 1  
VALUES OF  $y'_0(x')$  FOR THE NACA  $a = 1.0$  (UNIFORM PRESSURE) MEANLINE AT  $C_L = 1.0$

$x'$	0	0.1	0.2	0.3	0.4	0.5
$x'$	1.0	0.9	0.8	0.7	0.6	0.5
$y'_0(x')$	0	0.0299	0.0398	0.0486	0.0536	0.0532

The drag is assumed to consist solely of turbulent skin friction drag. Utilizing the velocity distribution as a function of  $C_L$ , Reference (1) shows that the drag coefficient is

$$C_d = 2 C_f \quad (20)$$

Also from the velocity distribution, Reference (1) shows that the critical cavitation number of the Region I forms is also the boundary expression between Regions I and II, which is

\*Called 2-term in view of the number of terms in a certain trigonometric series used in refining the pressure distribution

(Region I and II Boundary,  $M' = 0$ )  $\sigma = \frac{1}{2}C(21)$

and which is valid for  $C_L$  small relative to 1.6.

**Region II.** The general form of the cavitating hydrofoil family is shown by Reference (1) to be a supercavitating profile whose lower surface is fully wetted and whose upper surface is entirely covered by a cavity which springs from the leading edge.

The design of hydrofoil forms for  $a = 0$  is considered first. Utilizing the results of References (7), (8), and (9), the supercavitating forms which have lowest drag when  $\sigma = 0$  (for nearly all values of reasonable strength) is described by the parameters  $k$  and  $\delta$  of these references. The parameter  $k$  indicates the amount of Z-term camber\*, and  $\delta$  indicates the amount of thickness introduced by angle of attack where

$$k = 0.875 C_{L0} \quad (22)$$

$$\delta = 0.0787 C_{L0} \quad (23)$$

and where  $C_{L0}$  represents  $C_L$  when  $\sigma = 0$ .

The upper and lower coordinates of the hydrofoil surface (assuming that the hydrofoil just fills the cavity) are

$$\begin{aligned} (y'_u = 0) \quad y'_u &= y'_1(x') \cdot k + y'_3(x') \cdot \delta \\ (M' = 0) \quad y'_l &= y'_2(x') \cdot k + y'_4(x') \cdot \delta \end{aligned} \quad (24)$$

where approximate values of  $y'_1(x')$  through  $y'_4(x')$  are obtained from (8) and presented in Table 2, together with the values for  $y'_5(x')$  which will be utilized later.

TABLE 2  
APPROXIMATE VALUES OF  $y'_1(x')$  THROUGH  $y'_5(x')$  FOR THE BASIC 2-TERM CAMBER,  $\delta$ -THICKNESS, AND PARABOLIC THICKNESS DISTRIBUTIONS DERIVED FOR  $\sigma = 0$  AND INFINITE DEPTH

$x'$	0.0	0.05	0.1	0.2	0.4	0.6	0.8	1.0
$y'_1$	0	0.009	0.07	0.030	0.053	0.073	0.091	0.107
$y'_2$	0	0.018	0.0	3.7	0.071	0.111	0.102	0.038
$y'_3$	0	0.10	0.16	0.25	0.39	0.50	0.59	0.68
$y'_4$	0	-0.05	-0.10	-0.20	-0.40	-0.60	-0.80	-1.00
$y'_5$	0	0.22	0.32	0.45	0.63	0.77	0.89	1.00

The next problem is to determine the best forms for points in Region II where  $\sigma > 0$ . Although both nonlinear and linearized theories exist for determining the lower surface shape, cavity shape, and lift and drag coefficients for the case when  $\sigma > 0$  (Wu, References 10 to 12), the results would require a lengthy computer study to determine which form has the lowest drag for a given  $C_L$ ,  $\sigma$ , and strength.

A relatively simple solution to this problem is to linearly add the appropriate NACA  $a = 1.0$  uniform pressure meanline to the appropriate two-term supercavitating hydrofoil form (and cavity) designed for  $\sigma = 0$ . The result is a minimum drag

hydrofoil form for  $\sigma > 0$ . Letting  $\sigma$  be the incipient cavitation number of an NACA  $a = 1.0$  meanline, and  $C_L$  be the lift coefficient of a 2-term hydrofoil form at  $\sigma = 0$ , the lift coefficient  $C_L$  of the linearized combination is approximately

$$\text{(Region I)e } C_L - C_{L0} = 2\sigma \quad (25)$$

where  $C_L$  is assumed small; Region II is now called Region Iie for reasons which will be presented later. Notice that the pressure along the upper surface of the linearized combination, which shall be called the Region Iie form, is exactly cavity pressure when  $\sigma = \sigma_c$ . The nondimensional pressure along the lower surface is approximately the nondimensional pressure at  $\sigma = 0$  for the 2-term hydrofoil designed for  $C_L = C_{L0}$  plus the pressure  $\sigma_{cr}$ .

Notice that the NACA  $a = 1.0$  meanline is designed for a lift coefficient of  $C_L = C_{L0} = 2\sigma$ .

The Region Iie forms are seen to satisfy the necessary boundary conditions for minimum drag, which are: (1) the upper surface pressure is uniform and matches the cavity pressure, (2) the lower surface is fully wetted, and (3) the resulting form has minimum thickness and minimum cavity drag. Furthermore, the Region Iie forms are seen to merge into the Region I forms at the boundary between Regions I and Iie, since  $C_{L0} = 0$  along the boundary line where  $C_L = 2\sigma$ . Therefore, the Region Iie forms change smoothly from supercavitating 2-term forms designed for  $\sigma = 0$  to the NACA  $a = 1.0$  meanlines corresponding to the boundary line  $\sigma = C_L/2$ .

The nondimensional heights of the upper cavity wall and the lower hydrofoil surface  $y'_u$  and  $y'_l$  respectively, are

$$y'_u = y'_1(x') \cdot k + y'_3(x') \cdot \delta + y'_0(x') \cdot 2\sigma \quad (26)$$

(Region Iie)

$$y'_l = y'_2(x') \cdot k + y'_4(x') \cdot \delta + y'_0(x') \cdot 2\sigma$$

Equation 26 is valid only for low values of  $C_L$  because of the assumptions made in the linearized theory; Reference (9) reports negligible error up to  $C_L = 0.2$ , but considerable error may exist for  $C_L > 0.6$ . Therefore, the value of  $C_L$  in this analysis is limited to a maximum of 0.6.

The drag coefficient for the Region Iie forms is shown by (1) to be

$$C_d = 0.142(C_L - 2\sigma)^2 + \frac{0.236\sigma^2(C_L - 2\sigma)}{\sigma + 0.71(C_L - 2\sigma)} + C_f \left(1 - \frac{C_L}{2} + \frac{\sigma}{2}\right) \quad (27)$$

(Region Iie)

where the last term is friction drag and the other terms are cavity drag.

Illustration of the Resign Result. Some of the hydrofoil forms corresponding to the graph of  $\sigma$  versus  $C_L$  where  $M' = 0$  are shown superimposed on the lower graph of Figure 4 together with the boundary line between Regions I and Iie. The corresponding values of  $C_L$  are plotted in the upper graph. Only the cavity drag is plotted in Region Iie since  $C_L$  is negligible relative to  $C_L$  when  $R \gg 10^7$ . Values of  $C_L$  are plotted only up to 0.60 due to the limitations of the linearized theory. The most practical range of  $C_L$  for supercavitating hydrofoils is around 0.20, so the coverage is adequate.

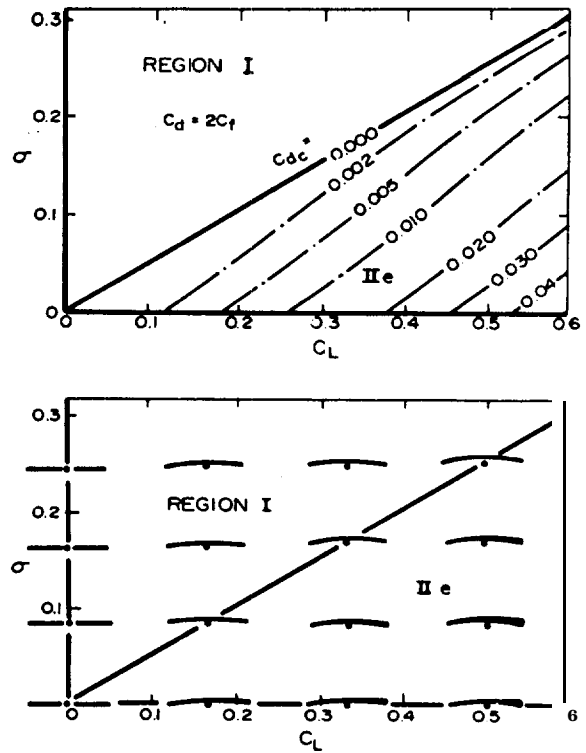


Figure 4 • Hydrofoil forms and drag coefficients for the case when  $M' = 0$

#### Resign Problem Where $\sigma = 0$

Since  $\sigma = 0$ , all points in the graph of  $C_L$  versus  $M'$  will correspond to supercavitating design forms consisting of different combinations of the 2-term camber configuration represented by  $k$ , parabolic thickness represented by  $\tau$ , and angle of attack thickness represented by  $\delta$ .

Reference (1) shows that Region II splits into the following families of supercavitating hydrofoils:

$$0.0502C_{L0}^2 \leq M' \begin{cases} k = 0 \\ \delta = (2/\pi)C_{L0} \\ \tau = 1.93 \sqrt{M' - 0.0014C_{L0}^2} - 0.426C_{L0} \end{cases} \quad (28)$$

(Region IIc)  
 $\sigma = 0$

$$0.0016C_{L0}^2 \leq M' \begin{cases} \tau = 0 \\ k = 0.962C_{L0} - 4.35 \sqrt{M' - 0.0012C_{L0}^2} \\ \delta = 0.024C_{L0} + 2.76 \sqrt{M' - 0.0012C_{L0}^2} \end{cases} \quad (29)$$

(Region IIId)  
 $\sigma = 0$

Solution of the Entire Three-Dimensional  
Design problem

$$\left( 0 \leq M' \leq 0.0016C_{Lo}^2 \right) \quad \begin{cases} \tau = 0 \\ k = 0.875C_{Lo} \\ \delta = 0.079C_{Lo} \end{cases} \quad (30)$$

where  $C_{Lo}$  is defined as

$$C_{Lo} = C_L - 2\sigma \quad (31)$$

The upper and lower surface coordinates are

$$\begin{cases} y'_u = y/(x') \cdot k + y'_3(x') \cdot \delta + y'_5(x') \cdot \tau \\ y'_l = y'_2(x') \cdot k + y'_4(x') \cdot \delta - y'_5(x') \cdot \tau \end{cases} \quad \begin{matrix} \text{(Regions IIc,} \\ \text{IIId, and IIe)} \end{matrix} \quad (32)$$

where the values of  $y'_1(x')$  through  $y'_5(x')$  are listed in Table 2.

The drag coefficient for all Region II forms when  $\sigma = 0$  is shown by (1) to be

$$C_d = \left[ 0.319k + 1.25(\tau + \delta) \right]^2 + C_f \left( 1 - \frac{C_{Lo}}{2} \right) \quad \begin{matrix} \text{(Region II} \\ \sigma = 0) \end{matrix} \quad (33)$$

The lower graph of Figure 5 illustrates the design result where  $\sigma = 0$ , and  $M'$  is plotted against  $C_L$ . Sketches of the corresponding design forms are superimposed. The upper graph of Figure 5 shows the values of the cavity drag coefficient, which is Equation 33 less the last term.

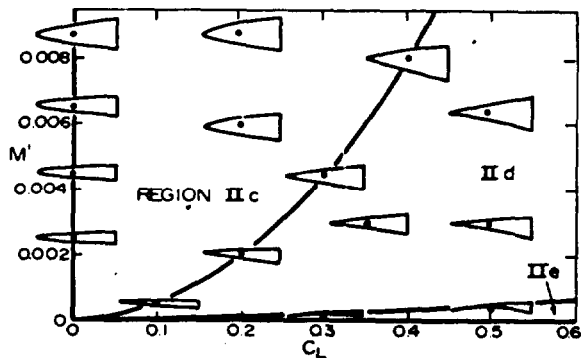
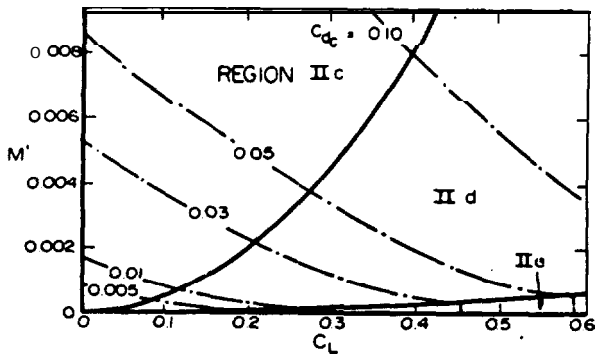


Figure 5. Hydrofoil forms and drag coefficients for the case when  $\sigma = 0$ .

The solutions to the three previous two-dimensional design problems can be used as guides in solving the three-dimensional problem represented by the three coordinates,  $C_L$ ,  $M'$ , and  $\sigma$ . The same physical equations are used, and the same general design concepts are applied: The expressions for the hydrofoil forms, their drag coefficients, and the boundaries between regions I, IIa, IIb, IIc, IIId, and IIe in the three-dimensional space of  $C_L$  versus  $M'$  versus  $\sigma$ , will be presented later. The boundaries, as derived in Reference (1), are shown in Figure 6, and the corresponding hydrofoil forms are shown superimposed in five different planes of the three-dimensional space in Figure 7. Notice how the hydrofoil forms change continuously between any two points in the three-dimensional space,

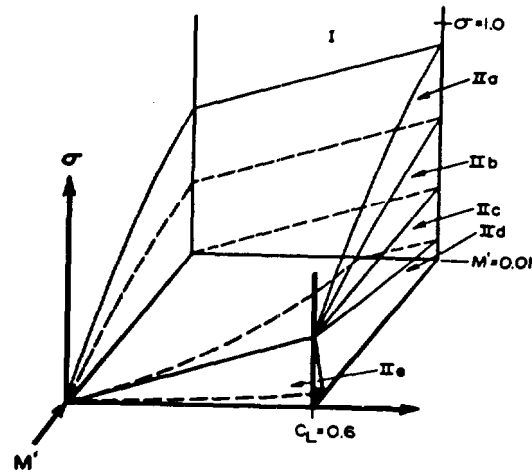


Figure 6 - Boundaries of Regions I through IIe in three-dimensional space

Transformation of the Three-Dimensional Design  
Problem into a One-Dimensional Design Problem

As a result of solving the three-dimensional design problem, Reference (1) shows that a significant simplification takes place by introducing the parameter K where

$$K = \frac{\sigma - C_L/2}{\sqrt{M'}} \quad (34)$$

Alternatively, K may be expressed as

$$K = \frac{\sigma}{f} \quad (35)$$

or

$$K = - \frac{C_{Lo}}{2\sqrt{M'}} \quad (36)$$

The equations for the region boundaries are expressed solely as a function of K in Table 3.

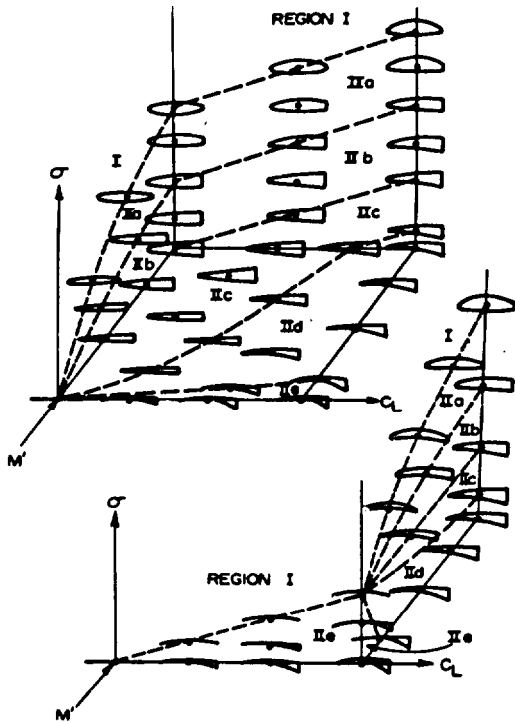


Figure 7 - Illustration of the solution to the three-dimensional design problem

TABLE 3  
REGION BOUNDARIES FOR SUBSPACE ( $\tau$ ) AS A FUNCTION OF  $K$

Region Boundary	Equation
I to IIa	$\sigma = 6.39$
IIa to IIb	$K = 3.19$
IIb to IIc	$K = 0$
IIc to IId	$K = -2.23$
IIe to IIe	$K = -12.5$

The simplification introduced for the description of the boundaries can be extended to the description of the hydrofoil forms and the drag coefficients. The following definitions are introduced:

$$\begin{aligned}
 \bar{c}_L &= c_L / \sqrt{M^T} \\
 \bar{\sigma} &= \sigma / \sqrt{M^T} \\
 \bar{y}' &= y' / \sqrt{M^T} = (y/c) / \sqrt{M^T} \\
 \bar{t}' &= t' / \sqrt{M^T} = (t/c) / \sqrt{M^T} \\
 \bar{\delta} &= \delta / \sqrt{M^T} \\
 \bar{\tau} &= \tau / \sqrt{M^T} \\
 \bar{k} &= k / \sqrt{M^T}
 \end{aligned} \tag{37}$$

\*Notice the difference in definition between the lower case  $k$  and the capital  $K$  symbols in Table 4.

$$\begin{aligned}
 \bar{c}_{dc} &= c_{dc} / M^T \\
 \bar{c}_{do} &= c_{do} / M^T
 \end{aligned} \tag{37}$$

where

$$c_{dc} = c_{do} + \frac{\frac{\pi}{4} \left( \frac{\sigma}{c} \frac{t}{c} \right)^2}{\sigma \frac{t}{c} + 1.5 c_{do}} \tag{38}$$

Equation 38 is an empirical relationship developed in (1) from the theory presented in References (13) and (14).

The hydrofoil forms as a function of  $K$ ,  $C_L$ , and the new variables defined by Equation 37 are listed in Table 4\*. The values for  $C_L$  are shown in Figure 2 as a function of  $K^2$ . The form and drag coefficients for the truncated ellipses of Regions IIa and IIb are presented in Figure 8. The expressions for  $C_L$  and the frictional drag coefficient  $C_{df}$  are listed for all hydrofoils in Table 5.

TABLE 4  
HYDROFOIL FORM CHARACTERISTICS

Region	Form Equation	$\bar{\tau} = \frac{t/c}{\sqrt{M^T}}$	$\frac{t_b}{t}$
I	$\bar{y}'_0 = 3.19 \sqrt{x'(x')^2 + y'_0 c'_L}$ $\bar{y}'_2 = -3.19 \sqrt{x' - (x')^2 + y'_0 c'_L}$	3.19	0
IIa	$\bar{y}'_0 = \frac{k}{2} \sqrt{\frac{2x'}{k/c_1} - (x')^2 + y'_0 c'_L}$ $\bar{y}'_2 = -\frac{k}{2} \sqrt{\frac{2x'}{k/c_1} - (x')^2 + y'_0 c'_L}$	$\frac{1}{\sqrt{c_1}}$	$k/c_1 \sqrt{\frac{2}{k/c_1} - 1}$
IIb	$\bar{y}'_0 = \frac{k}{2} \sqrt{\frac{1}{k^2 c_1} + 1} x' - (x')^2 + y'_0 c'_L$ $\bar{y}'_2 = -\frac{k}{2} \sqrt{\frac{1}{k^2 c_1} + 1} x' - (x')^2 + y'_0 c'_L$	$\frac{1}{\sqrt{c_1}}$	1.0
IIc	$\bar{y}'_0 = \gamma_1 \bar{k} + \gamma_2 \bar{\sigma} + 2\gamma_0 \bar{\sigma}$ $\bar{y}'_2 = \gamma_4 \bar{\sigma} - \gamma_3 \bar{\tau} + 2\gamma_0 \bar{\sigma}$ $\bar{k} = -1.272K$ $\bar{\tau} = 1.93\sqrt{1-0.0056K^2} + 0.85K$ $\bar{\sigma} = 0$	$-0.436K$ $+3.86\sqrt{1-0.0056K^2}$	1.0
IIe	$\bar{y}'_0 = \gamma_1 \bar{k} + \gamma_2 \bar{\sigma} + 2\gamma_0 \bar{\sigma}$ $\bar{y}'_2 = \gamma_2 \bar{k} + \gamma_4 \bar{\sigma} + 2\gamma_0 \bar{\sigma}$ $\bar{k} = -1.924K - 4.35\sqrt{1-0.0048K^2}$ $\bar{\sigma} = -0.048K + 2.76\sqrt{1-0.0048K^2}$ $\bar{\tau} = 0$	$-0.451K$ $+3.80\sqrt{1-0.0048K^2}$	1.0
IIe	$\bar{y}'_0 = \gamma_1 \bar{k} + \gamma_2 \bar{\sigma} + 2\gamma_0 \bar{\sigma}$ $\bar{y}'_2 = \gamma_2 \bar{k} + \gamma_4 \bar{\sigma} + 2\gamma_0 \bar{\sigma}$ $\bar{k} = -1.750K$ $\bar{\sigma} = -0.158K$ $\bar{\tau} = 0$	$-0.602K$	1.0

The basic form characteristics which consist of  $\bar{c}_L = (t/c)/\sqrt{M^T}$ ,  $t_b/t$ ,  $\bar{\tau}$ ,  $k/10$  and  $\bar{\delta}$  are plotted in Figure 9 as a function of  $K$ . Also shown in Figure 9 are typical hydrofoil shapes superimposed along vertical lines which represent the region boundaries. Notice how clearly and precisely Figure 9 presents all of the hydrofoil forms and how the

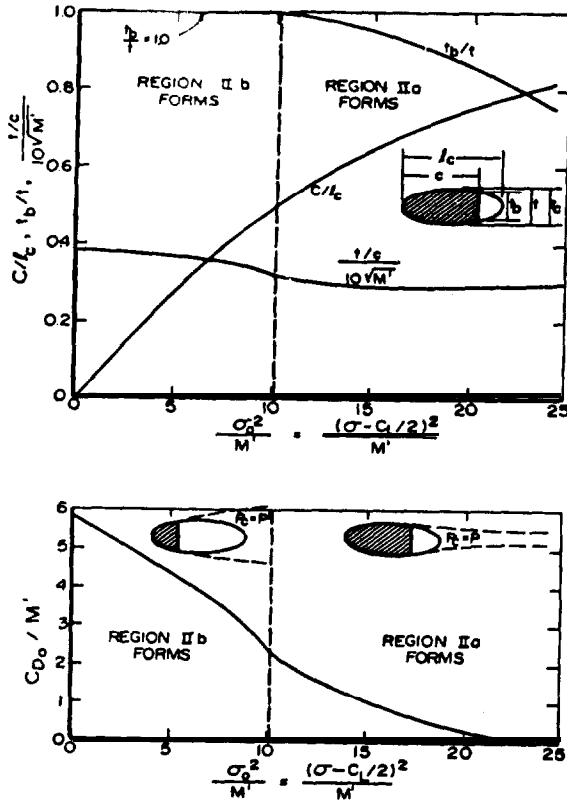


Figure 8 - Drag coefficients and physical properties of truncated ellipses

three-dimensional illustration in Figure 7 has been condensed into a single one-dimensional graph where the only parameter is  $K$ . The parameter  $K$  classifies all cavitating hydrofoils and the simpler fully-wetted hydrofoils much like the specific speed parameter classifies turbomachinery. The nature of the parameter  $K$  is somewhat broader than the specific speed parameter, however, because it includes the effect of cavitation and structural strength on design form which the latter &es not.

Figure 9 can be utilized together with Tables 4 and 5, Equations 57 and 38, and Figures 2 and 8, to completely specify the lowest-drag hydrofoil cross section as a function of  $C_L$ ,  $M'$ , and  $\sigma$ .

General Comments on the Design of Hydrofoil Cross Sections

The results of this hydrofoil design problem are applicable to a wide variety of operating situations. The restrictions that  $R \gg 107$  and  $r' = 0$  are not necessary as long as the boundary layer is turbulent; an expression for the frictional drag has been included to correct all drag coefficients for  $R$  and  $r'$ . No even the boundary layer state restriction is needed for the case of the cavitating Region II forms. The design assumption that there is negligible effect of the water surface on performance is also not important, in general, since very few hydrofoils are designed to operate steadily within about two chordlengths of the surface where depth affects become significant.

TABLE 5  
HYDROFOIL DRAG COEFFICIENTS

Region	$\bar{C}_{d0}$ (or $\bar{C}_{dc}$ )	$C_{dr}$
I	0	$2C_p(1+6.39 M')$
IIa	$\bar{C}_{dc} = \frac{c}{l} \frac{\sigma}{C_L M'}$	$C_p(1 - \frac{c}{2l} + \frac{c}{2l})^2$
IIb	See Figure 8	"
IIc	$2.41 - 1.0056K^2 - 0.525K^2$	"
IId	$2.06 - 1.0048K^2 - 0.674K^2$	"
IIe	$0.572K^2$	"

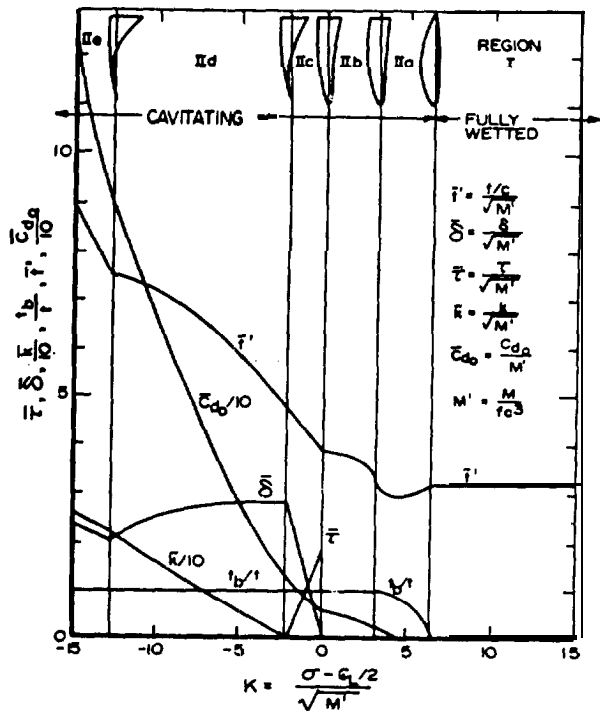


Figure 9 - One-dimensional representation of hydrofoil design form characteristics

The restriction that  $\Delta\alpha = 0$  can be relaxed to  $\Delta\alpha = \pm 3^\circ$  or more, in general, for fully-wetted hydrofoils when the boundary layer is turbulent, without seriously influencing the performance or design form, unless cavitation is very critical. The effect of short periods of positive values of  $\Delta\alpha$  on supercavitating hydrofoil performance or design form is small; however, if  $\Delta\alpha$  is to be negative, the upper surface should be undercut so that the cavity clears it at negative angles of attack. The restriction to solid sections is not serious because the designer can easily modify the specified  $M'$  to account for any amount of hollowness by using a fictitiously high value of  $M'$ . Similarly, the assumption that the separation drag of the fully-wetted hydrofoils is negligible can be complied with by adding a cusp-shaped or wedge-shaped trailing edge to reduce separation of the turbulent

boundary layer\*. A final **comment** is that the results of this analysis can also be **made** to apply to a relatively new kind of hydrofoil form **introduced** by Hydronautics, Incorporated, called a **super-cavitating** hydrofoil with an **annex**. (15) This form is **essentially** a typical Region II-hydrofoil form with an unwetted annex extending rearward into the cavity from the trailing edge to increase the bending strength without changing any of the performance characteristics. Such a **form can** be treated in this **analysis** by artificially **reducing** the **required** value of  $M'$  by perhaps thirty **percent** or whatever value the designer finds reasonable in view of the anticipated form of the hydrofoil and cavity. When the design of the Region II form has been completed, the designer can add the annex and check his earlier estimate of approximate annex size and strength. change. By applying these modifications, the selected conditions for this analysis are found to be significantly extended.

Notice that the hydrofoil forms split into six different families in which each family is described by a different set of equations. Although some of the families and their boundaries in **problem** space are uniquely **determined**, while the determination of others is arbitrary and depends upon the variables used in describing the hydrofoil form. For **example**, the boundary between Regions I and II is uniquely determined because it results from a **fundamental** change in physical flow condition. On the other hand, the boundaries between Regions **IId**, **IIf**, and **IIf** are not unique because instead of using the variables  $k$ ,  $r$ , and  $\delta$  to represent the **amount** of **two-term** camber, parabolic thickness distribution, and  $\delta$ -**thickness** distribution, other variables could have been used to represent other kinds of basic camber and thickness distributions. Essentially the same hydrofoil **form** would be **found** to correspond with each  $\delta$ -sign problem, but the equations  $\delta$ -scribing the forms would be different. Slight form changes and **small** improvements in performance will probably be found for Regions **IIf**, **IId**, and **IIf** as a result of further research into new forms. No changes are anticipated in the forms or boundary description corresponding to Regions I, **IIf**, and **IIf** within the framework of the stated **assumptions**. Also, the classification parameter  $K$  which resulted from this analysis should remain unique.

\*The low-drag hydrofoil **forms** are very close in shape to an ellipse with either a cusp-shaped or a wedge-shaped trailing edge. For example, see the NACA **16-series** and **65-series** airfoils of Reference (6). Also, a **sharp** trailing edge is necessary in order to **satisfy** the Kutta condition for the lifting hydrofoils: Notice that the value of  $M'$  reduces when such a trailing edge is added; this reduction in  $M'$  can be accounted for by reducing the specified value of chordlength about 20 percent, or whatever value appears reasonable for the thickness-to-chord ratio. Notice that the specified **value** of  $C$  has to be changed accordingly. This trailing edge **addition** affects only the Region I forms.

The author wishes to thank his advisor, Professor G. F. **Wislicenus**, for his generous assistance during the period when the **PhD** thesis was written. This paper is an abstract of a portion of that thesis.

References

1. Lang, T. G. "A Generalized Engineering Design Procedure," **PhD** Thesis, Department of Aerospace Engineering, Pennsylvania State University, University Park, Pennsylvania, June, 1968.
2. Tulin, **M. P.**, and **Burkart**, M. P. "Linearized Theory for Flows About Lifting Foils at Zero Cavitation **Number**," Report C-683, The David Taylor Model Basin, Washington, D. C., February, 1955.
3. **Tulin**, M. P. "Steady Two-Dimensional Cavity Flows About Slender Bodies," Report 834, The David Taylor Model Basin, Washington, D. C., May, 1953.
4. Lang, T. G. "Base-Vented Hydrofoils," NAVORD Report 6606, U. S. Naval Ordnance Test Station, China Lake, California, 19 October 1959.
5. Tulin, M. P. "The Shape of Cavities in Super-cavitating Flows," Technical Report 121-5, Hydronautics, Inc., Laurel, Md., April, 1965.
6. Abbott, **I.H.**, and **Von Doenhoff**, A. E. **Theory of Wing Sections**, New York: Dover **Publications**, Inc., 1959.
7. Johns, V. E., Jr. "Theoretical Determination of Low-Drag Supercavitating Hydrofoils and Their Two-Dimensional Characteristics at Zero Cavitation **Number**," NACA RML57G11a, September, 1957.
8. Auslaender, J. "The Linearized Theory for Supercavitating Hydrofoils Operating at High Speeds Near a Free Surface," **Journal of Ship Research**, October, 1962, 8-23.
9. **Auslaender**, J. "Low Drag Supercavitating Hydrofoil Sections," Technical Report 001-7, Hydroanautics, Inc., Laurel, Md., April, 1962.
10. Wu, T. Y. "A Free Streamline Theory for Two-Dimensional Fully **Cavitating** Hydrofoils," **J. Math. Phys.**, XXXV (1956), 236-65.
11. **Wu**, T. Y. "A Note on the Linear and Nonlinear **Theories** for Fully Cavitated Hydrofoils," California Institute of Technology **Hydro. Lab. Report**. Pasadena, California, 1956.
12. **Wu**, T. Y. "A Wake Model for Free-Streamline Flow **Theory**; Part I, Fully and Partially Developed Wake Flows and Cavity Flows Past an Oblique Flat Plate," **J. Fluid Mech.**, XIII (1962), 161-81.
13. **Fabula**, A. G. "Application of Thin-Airfoil Theory to Hydrofoils with Cut-off Ventilated Trailing Edge," **NAVWEPS Report** 7571, U. S. Naval Ordnance Test Station, China Lake, California, 13 September 1960.
14. **Fabula**, A. G. "Linearized Theory of Vented Hydrofoils," NAVWEPS Report 7637, U. S. Naval Ordnance Test Station, China Lake, California, 7 March 1961.
15. **Tulin**, M. P. "Supercavitating Flows - Small Perturbation Theory," Technical Report 121-3, Hydronautics, Inc., Laurel, Md., September, 1963.